



LAWRENCE
LIVERMORE
NATIONAL
LABORATORY

Electrostatic Breakdown Analysis using EMSolve and BEMSTER

Ben Fasenfest, Daniel White

June 6, 2005

Disclaimer

This document was prepared as an account of work sponsored by an agency of the United States Government. Neither the United States Government nor the University of California nor any of their employees, makes any warranty, express or implied, or assumes any legal liability or responsibility for the accuracy, completeness, or usefulness of any information, apparatus, product, or process disclosed, or represents that its use would not infringe privately owned rights. Reference herein to any specific commercial product, process, or service by trade name, trademark, manufacturer, or otherwise, does not necessarily constitute or imply its endorsement, recommendation, or favoring by the United States Government or the University of California. The views and opinions of authors expressed herein do not necessarily state or reflect those of the United States Government or the University of California, and shall not be used for advertising or product endorsement purposes.

This work was performed under the auspices of the U.S. Department of Energy by University of California, Lawrence Livermore National Laboratory under Contract W-7405-Eng-48.

Electrostatic Breakdown Analysis Using EMSolve and BEMSTER

Benjamin Fasenfest

Daniel White

Feb. 15, 2005

I. Introduction

Computer simulations modeling electrostatic behavior were used to simulate dielectric breakdown problems. These simulations modeled composite dielectric and conducting structures to see how much voltage difference or charge accumulation could occur before dielectric breakdown occurred in an air region. Two different computer codes were used for the analysis; EMSolve and BEMSTER. EMSolve, an existing LLNL internal finite element code, requires that a complete volume mesh of the problem be constructed. BEMSTER, a boundary-element code, was developed from an extension of the FEMSTER libraries which power EMSolve. The boundary-integral code offers the advantages of solving for accumulated charge and maximum electric field directly, and of only requiring a surface mesh. However, because it does not automatically solve for the voltage and electric field everywhere in space, post-processing and visualization are slightly more difficult than with EMSolve. Both codes were compared to several analytical solutions, and then applied to the structures of interest. Both codes showed good agreement with the analytic solution and with each other.

II. BEMSTER Overview

The BEMSTER Electrostatic software requires that all geometry structures are of one of two types: An infinitesimally thin conducting sheet, or a closed dielectric body. It satisfies two boundary conditions; one for perfect conductors and one for closed

dielectric bodies. The overall formulation is very similar to that of [1] [2], and [3]. On conductors, it satisfies

$$V(\mathbf{r}) = \frac{1}{4\pi\epsilon_0} \int_S \frac{\sigma(\mathbf{r}')}{|\mathbf{r} - \mathbf{r}'|} ds', \quad (1)$$

Where V is the known voltage on the conductor and σ is the total charge on the source surface. This total charge is the sum of free charge and polarization charge at dielectric interfaces. The surface is triangulated into quadrilaterals or triangles, and the charge is represented in terms of differential forms 2-form basis functions as

$$\sigma(\mathbf{r}') = \sum_{n=1}^N I_n \Pi_n. \quad (2)$$

Testing equation 1 using the Galerikin method, the matrix system

$$[Z_c][I_c] = [V_c] \quad (3)$$

can be constructed where

$$Z_{mn} = \langle \Pi_m, G, \Pi_n \rangle \quad (4)$$

with

$$G = \frac{1}{4\pi\epsilon_0 R}. \quad (5)$$

On dielectric boundaries, the jump condition

$$\epsilon^+ \mathbf{E}^+(\mathbf{r}) \cdot \hat{\mathbf{n}} = \epsilon^- \mathbf{E}^-(\mathbf{r}) \cdot \hat{\mathbf{n}} \quad (6)$$

needs to be satisfied, where the + and – denote the outside and inside of the dielectric with respect to its surface normal. Equation (6) can be re-written in terms of an integral over all surfaces as

$$\frac{(\epsilon_r^- + \epsilon_r^+)}{2(\epsilon_r^- - \epsilon_r^+)} \sigma(\mathbf{r}) + \frac{1}{4\pi\epsilon_0} \int_S \frac{(\mathbf{r} - \mathbf{r}') \cdot \mathbf{n}}{R^3} \sigma(\mathbf{r}') d\mathbf{r}' = 0. \quad (7)$$

The first term in equation 7 is only present when the test and source patches are the same; the second term is only present when the test and source patches are not the same. This leads to the matrix equation for the complete system of conducting and dielectric bodies:

$$\begin{bmatrix} Z_{cc} & Z_{cd} \\ K_{dc} & \frac{1}{2\lambda} + K_{dd} \end{bmatrix} \begin{bmatrix} \sigma_c \\ \sigma_d \end{bmatrix} = \begin{bmatrix} V_c \\ 0 \end{bmatrix}, \quad (8)$$

Where

$$K_{mn} = \langle \Pi_m, \nabla \cdot \mathbf{G}, \Pi_n \rangle \quad (9)$$

and

$$\frac{1}{2\lambda} = \frac{(\epsilon_r^- + \epsilon_r^+)}{2(\epsilon_r^- - \epsilon_r^+)} \Pi_m. \quad (10)$$

A symmetry ground plane can be implemented without adding to the mesh by changing the Green's function. The new Green's function automatically adds the contribution from the reflected source. For a PEC ground plane at $z=0$, the Green's function becomes

$$G = \frac{1}{4\pi\epsilon_0} \left(\frac{1}{|\mathbf{r} - \mathbf{r}'|} - \frac{1}{|(r_x - r'_x)\hat{\mathbf{x}} + (r_y - r'_y)\hat{\mathbf{y}} + (r_z + r'_z)\hat{\mathbf{y}}|} \right). \quad (11)$$

With these equations implemented, running a problem using BEMSTER requires the following steps:

- 1) Mesh the surfaces of all dielectric objects as well as all conductors

- 2) Determine which side of dielectric bodies is in the normal direction
- 3) Enter the dielectric constants above and below every dielectric interface
- 4) Enter the voltage on every conducting surface
- 5) Indicate the existence of a PEC ground plane

BEMSTER then solves for the total charge on the surfaces, which can be used to determine the total charge as well as voltage and electric field values at any point in space.

III. Code Verification

To test both the BEMSTER and EMSolve codes, several problems with known analytic solutions were run. The first of these consisted of two concentric PEC spheres, shown in Figure 1.

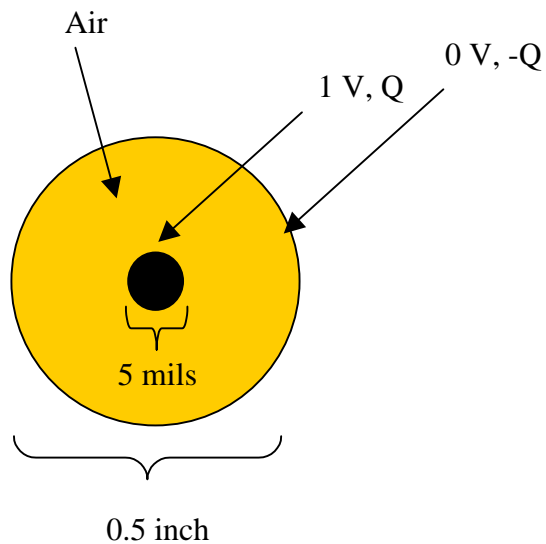


Figure 1. Two concentric air-filled conducting spheres. The inner sphere has a potential of 1 V with respect to the outer sphere.

The exact solution for the electric field strength can be found from Gauss' Law as

$$E = \frac{V}{\left(\frac{1}{a} - \frac{1}{b}\right)r^2} \quad (12)$$

giving a total charge on the inner conductor of:

$$Q = \frac{4\pi\epsilon V}{\left(\frac{1}{a} - \frac{1}{b}\right)} = 7.1367e-15 \text{ C} \quad (13)$$

The problem was meshed using 640 quads on the inner sphere and 864 quads on the outer sphere. The charge Q was $7.0992e-15$ C, for an error of 0.525%. The problem was meshed for EMSolve with 76,800 hexahedron. A plot of the voltage in a cross-section of the sphere is shown in Figure 2.

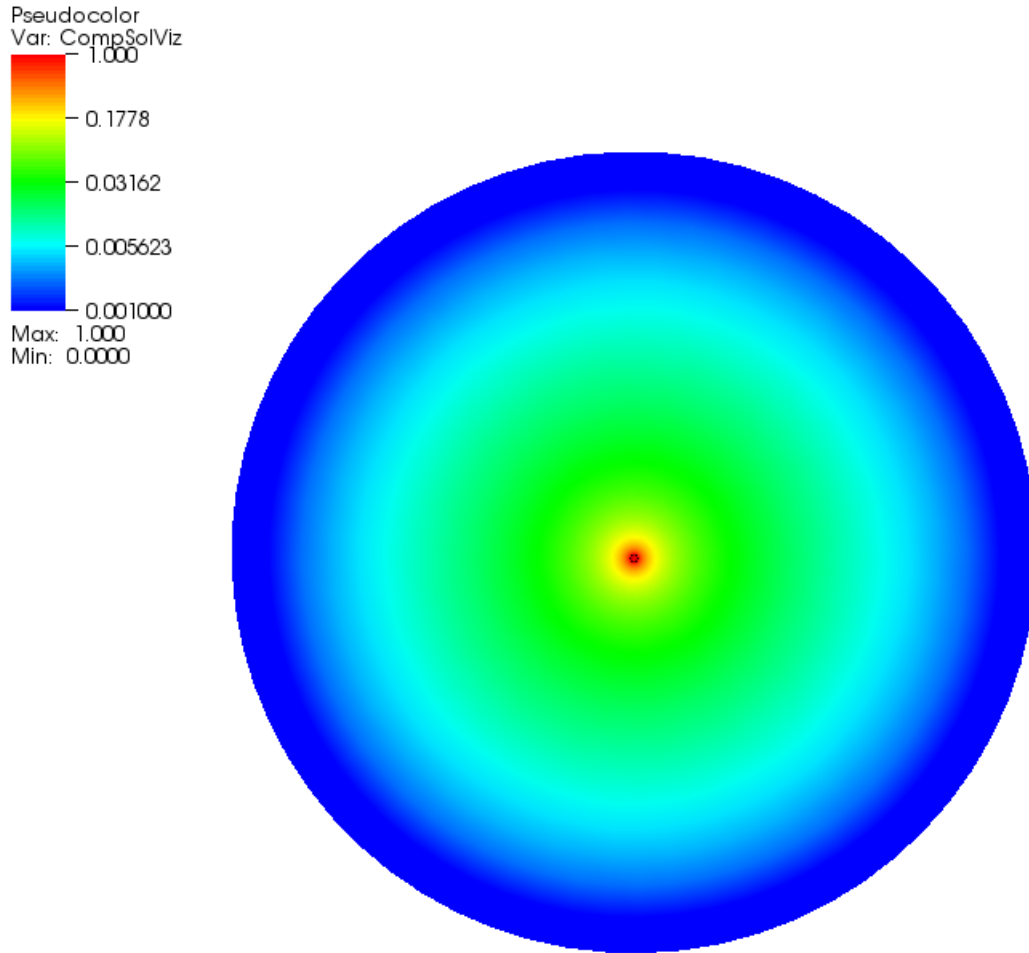


Figure 2. Voltage between the two conducting spheres, as computed by EMSolve.

The voltage solution for both simulations was compared with the exact solution, and the error plotted in Figure 3. Both codes showed good agreement, with the EMSolve code performing slightly better. This is likely due to the increased mesh density used for the EMSolve simulation.

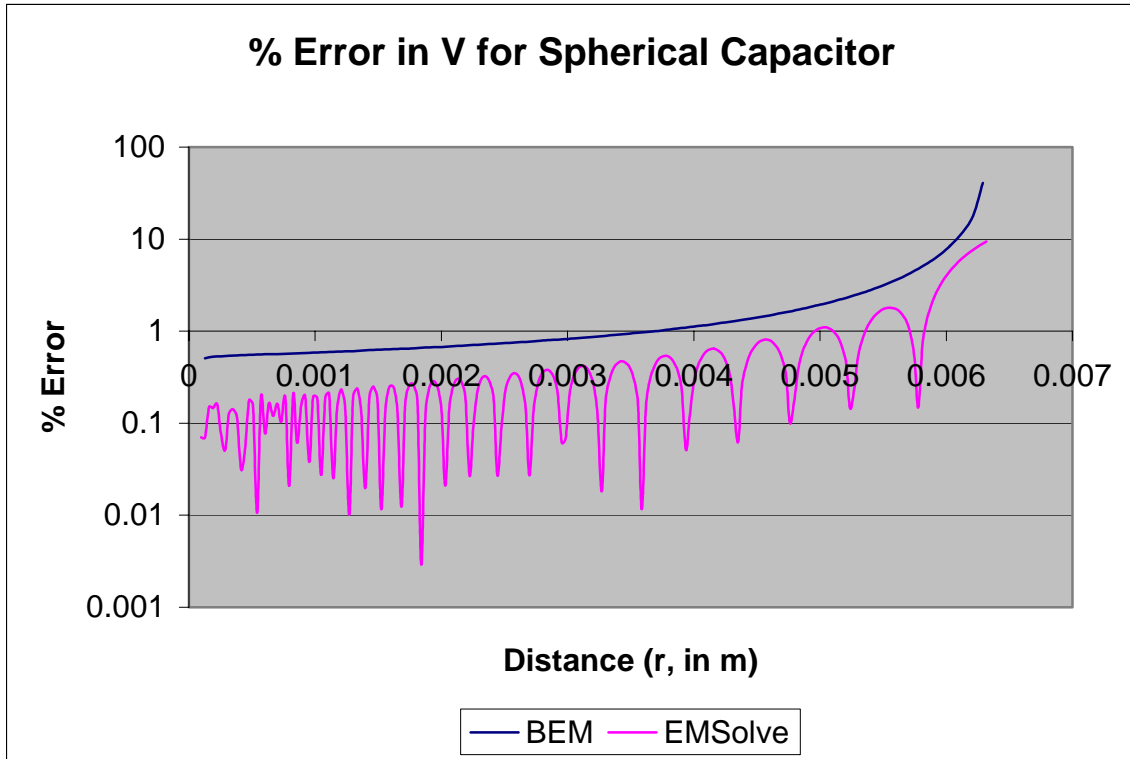


Figure 3. Comparison of the error for the BEMSTER and EMSolve codes for the concentric spheres.

The second test case consisted of two hemispheres over a perfect ground plane. This arrangement is shown in Figure 4. By applying symmetry, the ground plane can be removed, and the voltages reflected across it. Because the original structure has a 1 V potential on the inner hemisphere and a 0 V potential (grounded) on the outer hemisphere, the voltage on the reflected inner hemisphere is -1 V, while the voltage on the reflected outer hemisphere remains at 0 V.

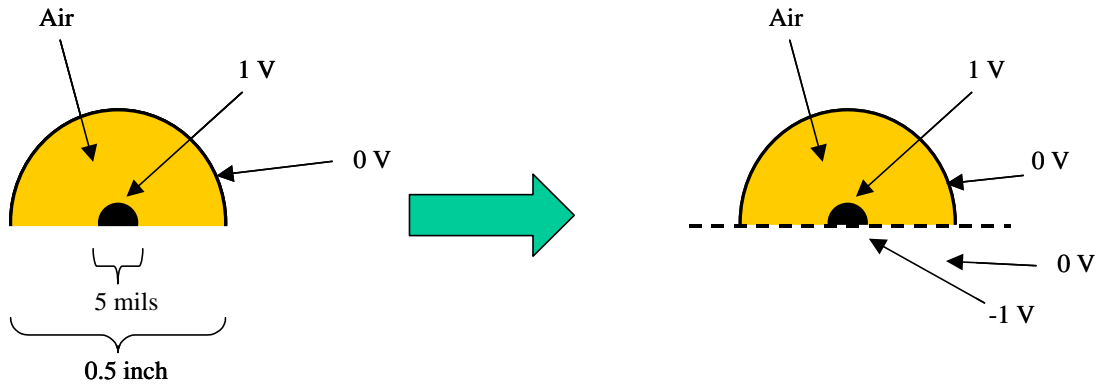


Figure 4. Concentric hemispheres, before and after symmetry is applied.

An analytic solution for this problem was written in Mathcad. It relies on a series expansion, and hence is not exact, although as more terms are kept it approaches the exact solution. The electric field along the ground plane was compared for the two codes and analytic solution. A plot of this electric field is shown in Figure 5. Both codes do a good job of matching the analytic solution. Both codes have their greatest error near the outer surface, where the electric field strength is very small. This could be due to numerical precision errors. However, it is unlikely to become important in dielectric breakdown problems, where the region of maximum electric field is the most important.

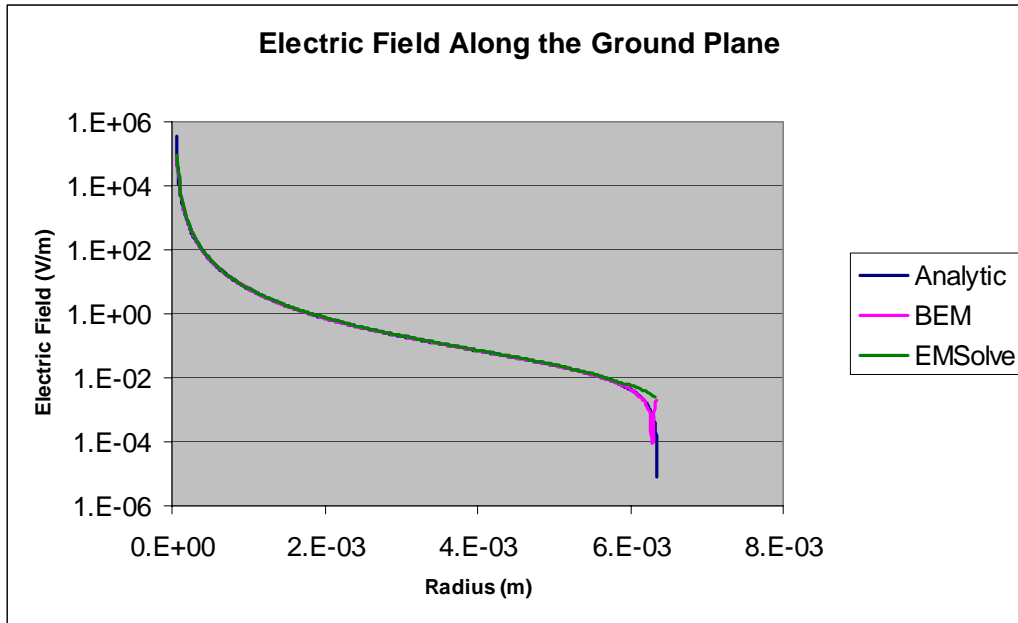


Figure 5. Electric field strength along the ground plane between the inner and outer spheres.

IV. Results for Problems of Interest

Dielectric-coated Box Above Ground Plane

The first problem of interest simulated was that of a dielectric-coated conducting box above a ground plane. The geometry for this structure is shown in Figure 6.

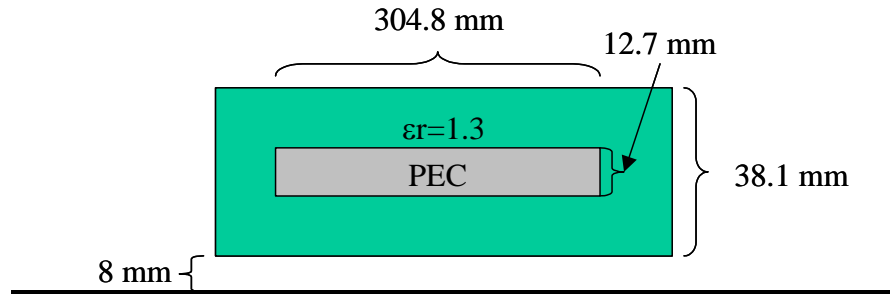


Figure 6. The PEC box has dimensions 304.8mm x 228.6mm x 12.7 mm. The dielectric surrounding it is 12.7 mm thick. The bottom of the dielectric is 8 mm above the ground plane.

This structure can be modeled analytically as a parallel plate capacitor, neglecting the fields due to fringing and assuming charge build-up only occurs on the bottom of the PEC box. Under these assumptions, if the PEC box has a potential of 1 V with respect to the ground plane, the maximum electric field strength in the air region would be 56.2789 V, and there would be 3.4721×10^{-11} C of charge on the box. Assuming a breakdown voltage in air of 3×10^6 V/m, these results imply that the box could hold 1.85×10^{-6} C of charge or have a potential of 53.308 kV before breakdown would occur in the air region.

A volume mesh was created for the structure and simulated in EMSolve. The computed electric field is shown for a cross section of the mesh in Figure 7. This cross section is taken down the center of the box in y. As expected, the electric field is mostly contained directly beneath the metal box, between the box and the ground plane.

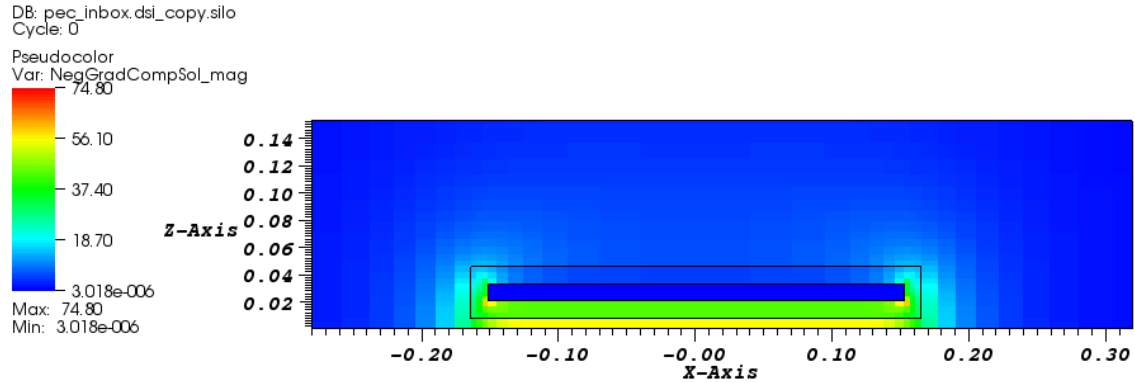


Figure 7. Electric field magnitude in a cross-section of the problem.

The peak field strength in the air region from EMSolve is 56.28 V/m, while the peak field strength in the dielectric is 74.80 V/m. Assuming a breakdown voltage of 3 MV/m for air, the necessary ground-box potential would be 53.21 kV.

The BEMSTER code was also used to test the pec in the dielectric box. The symmetry Green's function was used to represent the ground plane, so that only the surface of the PEC and surface of the dielectric needed to be meshed. A much simpler mesh was used than for the FEM model, consisting of only 1320 patches. This mesh was ran using 0th order bases with centroid testing. The total charge on the box was calculated to be 5.31e-11, compared to the parallel-plate model value of 3.47e-11. The likely reason for the greater amount of charge is the increased surface area of a box rather than the plate used in the analytic model. On a box, some charge will be on the top and sides of the box as well as on the bottom of the box.

With the maximum electric field strength in the air region assumed to be directly beneath the center of the box (56.292 V/m), the necessary voltage for breakdown at 3e6 V/m is 53.29 kV. The charge on the box for this voltage is 2.83e-6 C, compared to 1.85e-6 C from the simple analytic model. The results for the electric field in a line up through the center of the box is compared for EMSolve and BEMSTER in Figure 8.

Both show good agreement, with distinct field strengths beneath the box, no field within the box, and a slowly decreasing field above the box.

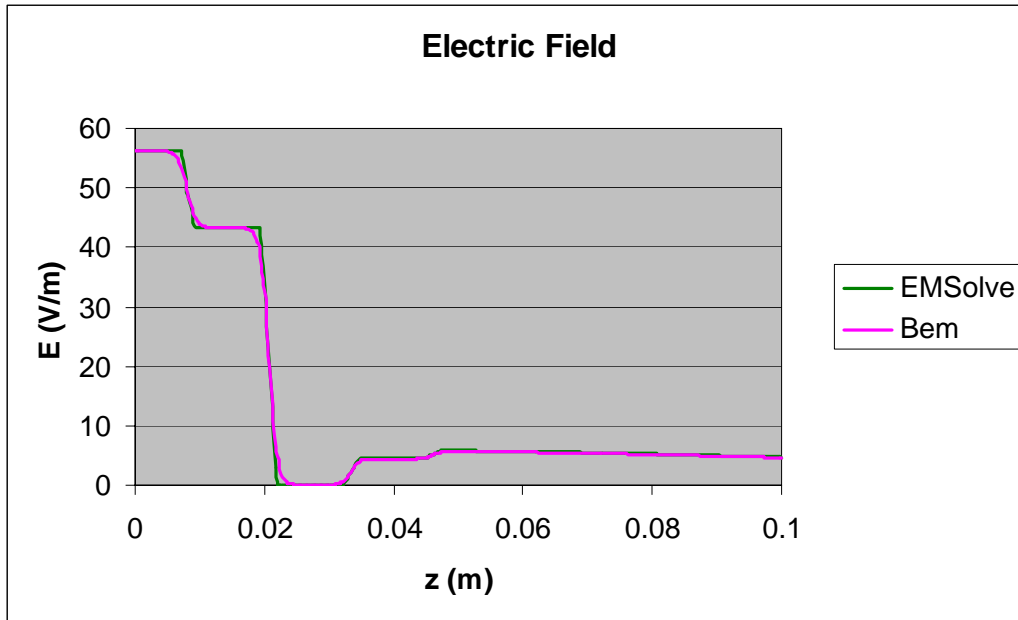


Figure 8. Electric field strength in a line up through the center of the box.

For the next set of tests, the dielectric was removed from the $-x, +z$ quarter of the dielectric block, exposing the metal in this area. This change does not affect the simplified analytic model. However, it does change the field distribution somewhat, as seen in Figure 9. The electric field is greater on the top of the plate at the left side.

The electric field under the plate is 56.277 V/m, unchanged from the case with the complete dielectric. The maximum electric field in the air below the plate is 56.28 V/m, again unchanged. However, the maximum in the air in the missing chunk is 70.28 V/m, giving a breakdown potential of 42.68 KV. This is due to the presence of 2 sharp PEC corners in the upper air region. The location of these hotspots can be seen in Figure 9, which shows the air region where the dielectric is missing. The grid lines represent the

mesh of the metal plate. The hot spots, shown in orange, are where the electric field intensity is greatest in the air.

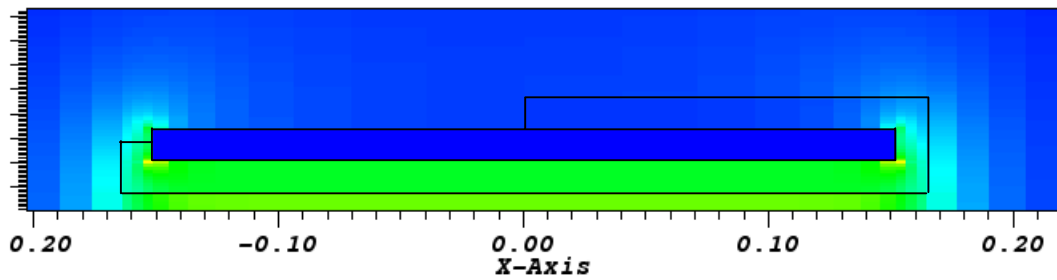


Figure 9. Electric field with $\frac{1}{4}$ of the dielectric missing.

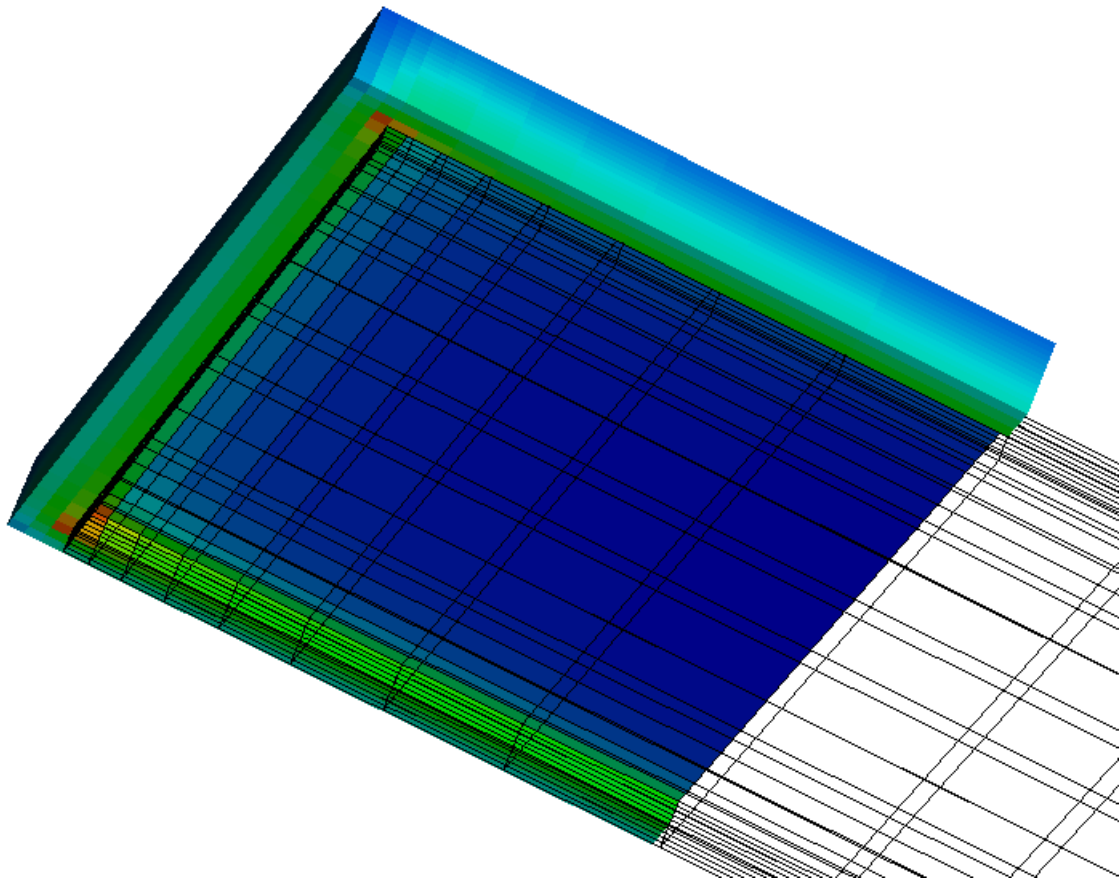


Figure 10. Electric field strength in the missing dielectric region. The highest E-field occurs near the corners of the metal box where the dielectric has been removed.

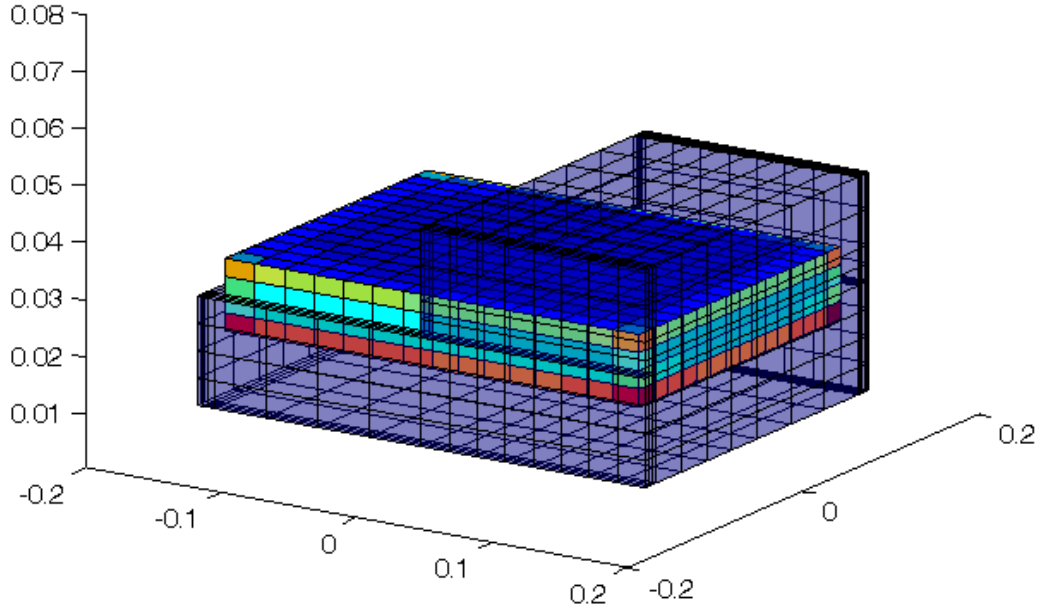


Figure 11. Charge density on the PEC box. The dielectric is shown surrounding it. The charge shown is total charge, not free charge. Charge buildup can be seen on the bottom of the box and on the corners, as expected.

The maximum electric field in the air region for the BEM simulation can be approximated from the boundary condition

$$\mathbf{E} \cdot \hat{\mathbf{n}} = \frac{\rho_t}{\epsilon_0} \quad (14)$$

where only the patches in the air region of the conductor are checked for maximum ρ_t (total charge density). This equation assumes that there is no polarization charge on the conductors, which will be true as long as the conductor forms a closed body rather

than a thin sheet between dielectric layers. Using this measure, the maximum electric field strength is found to be 105.01 V/m near the corners in the air region. However, as the charge (and electric field) are singular at the corners, this value may be due more to discretization than to geometry. Total charge on the conducting box is $5.33e-11$ C.

The problem was re-meshed with rounded corners and edges. Rounding radii of 2mm and 4mm were simulated. This resulted in a very large number of elements. The results for the electric field from EMSolve for rounded corners is shown in Figures 12 and 13. The result is very similar to that in Figure 8 with the missing dielectric and no rounding. The maximum E-field in the air region is 56.28 V/m, the same as for the case with unrounded corners. It can be assumed that the rounding of the corners only lowers the electric field right at the corners, and does not have much affect on the electric field by the time it enters the air region.

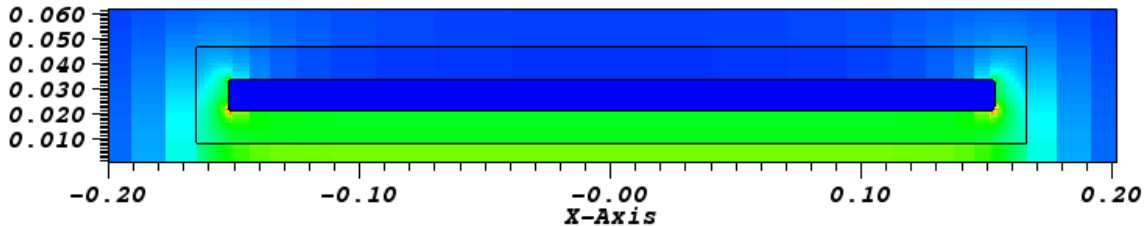


Figure 12. E-field magnitude with 2 mm radius edge rounding

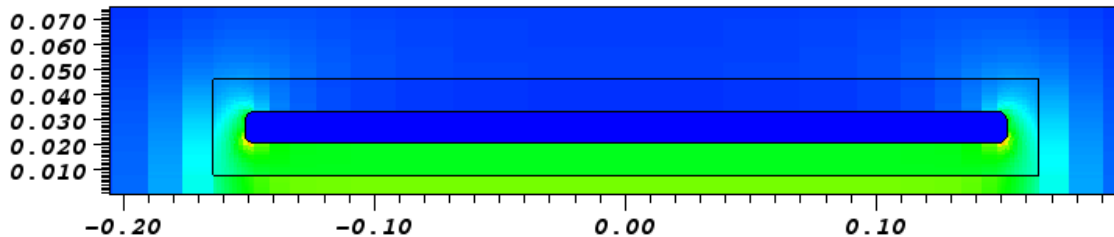


Figure 13. E-field magnitude with 4 mm radius edge rounding

The results for the breakdown voltages for the dielectric coated box are summarized in Table 1.

Table 1: Results for the breakdown voltage for the dielectric-coated box

Structure	<i>Parrallel Plate Model</i>	<i>EMSolve BEMSTER</i>	
Square corners, complete dielectric	53.31 kV	53.21 kV	53.29 kV
Square corners, missing dielectric	-	42.68 kV	28.57 kV
Rounded corners, complete dielectric	53.31 kV	53.21 kV	53.29 kV

PEC Nubs above a Dielectric

The geometry for this problem is shown in Figure 14. The problem consists of an air-filled hemisphere over a dielectric cylinder. The outside walls of both the hemisphere and cylinder are assumed to be PEC. Two hemispherical nubs lie on top of the dielectric. They are excited to +1 V and -1 V, respectively, while the outside conducting shell is considered grounded at 0 V. The maximum electric field in the air region is desired for dielectric breakdown considerations.

The hardest part about simulating this problem was generating a suitable mesh. It was fairly straight forward to generate a mesh for use with BEMSTER, as only surfaces needed to be meshed correctly. This allowed easy mesh creation with both TruGrid and CUBIT. However, the mesh generation for EMSolve, which required a quality volume mesh, was much more difficult. A reasonable, if somewhat coarse, mesh was finally generated using CUBIT, which allows for tetrahedral meshing.

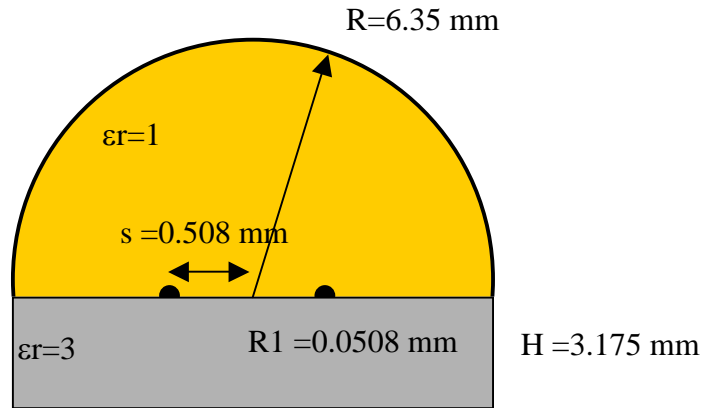


Figure 14. Geometry for the problem

A rough plot of the electric field cross section is shown in Figure 15. This electric field was determined from BEMSTER. It can be seen that the magnitude of the electric field is not greatly affected by the presence of the dielectric layer. This can be confirmed by viewing a similar plot of the electric field strength from Maxwell3D, a commercial finite element code, shown in Figure 16. The problem was also simulated in EMSolve using a coarse tetrahedral mesh, plotted in Figure 17. Figures 18,19, and 20 show the electric field around a single nub. Figure 21 compares the electric field strength in a line up through the center of one nub. As can be seen, all three codes agree fairly well.

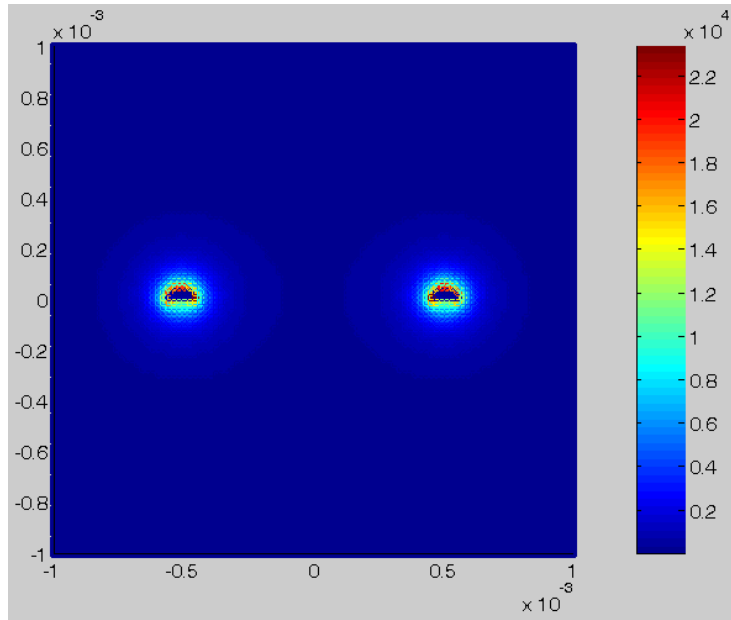


Figure 15. Magnitude of the electric field in the plane containing the two dielectric hemispheres.

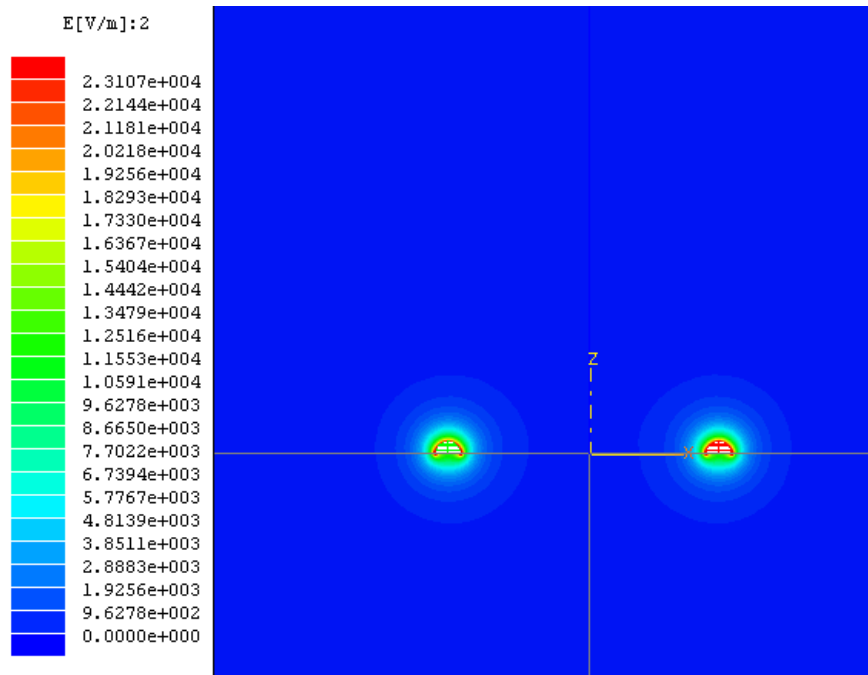


Figure 16. Side view from Maxwell3D. The qualitative behavior of the fields is similar.

The maximum value of the colorscale is the same as for the BEM plot, although the colormap is different.



Figure 17. Side view from EMSolve using a relatively coarse tetrahedral mesh.

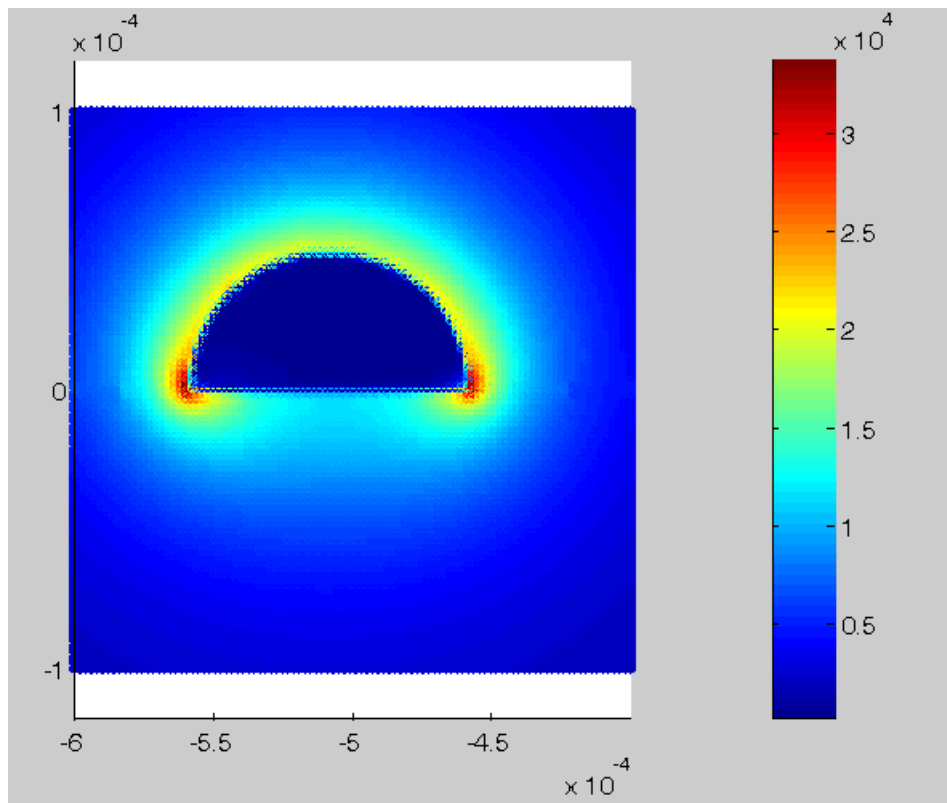


Figure 18. BEMSTER solution for the electric field magnitude around one of the PEC nubs.

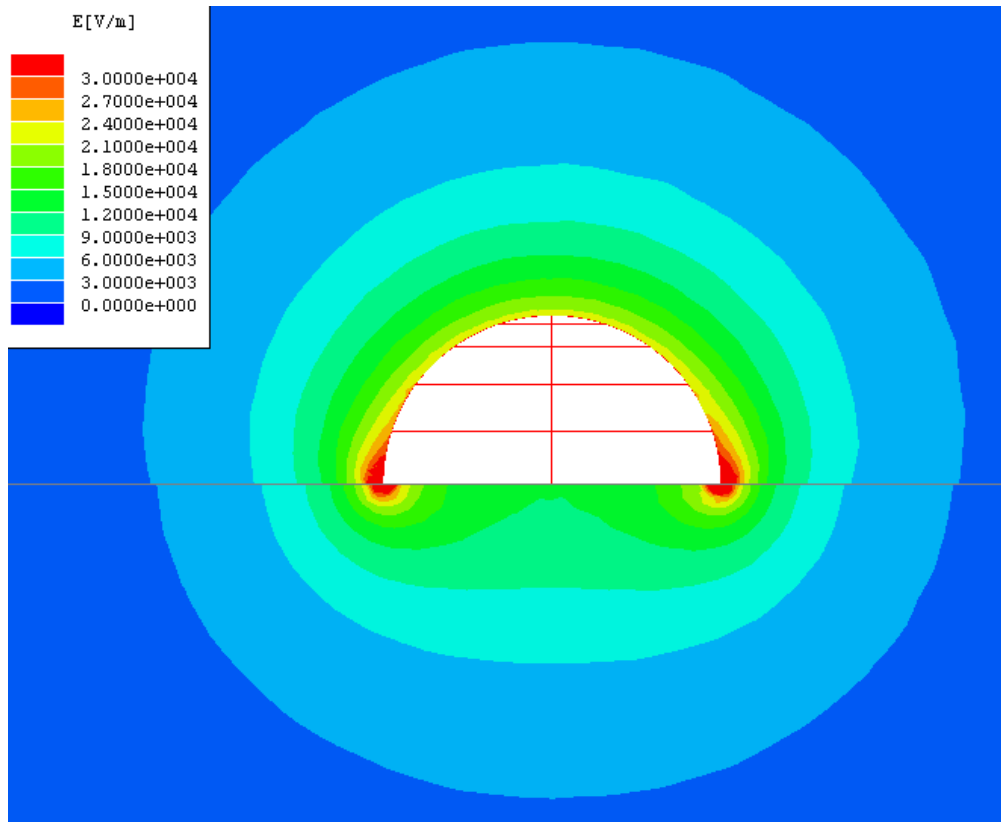


Figure 19. Maxwell3D electric field around one of the PEC nubs

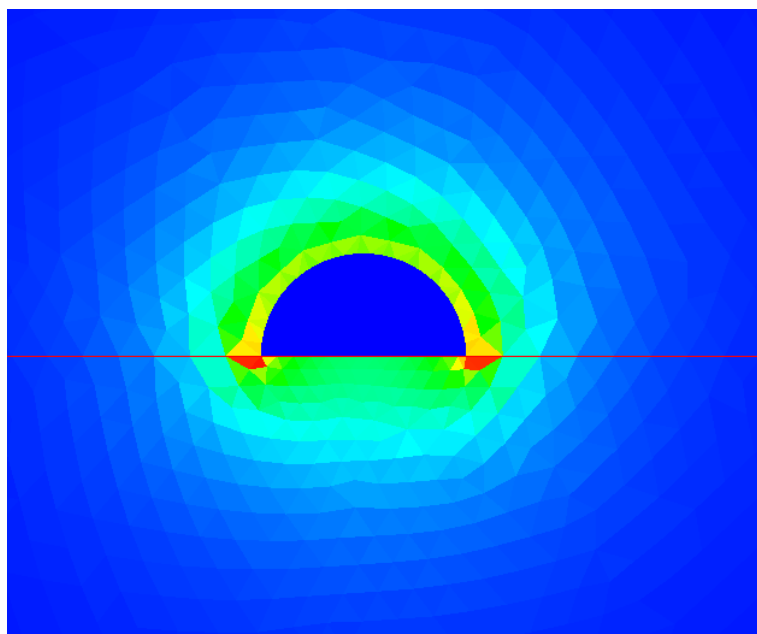


Figure 20. EMSolve solution for the electric field around one of the nubs. The red line marks the surface of the dielectric.

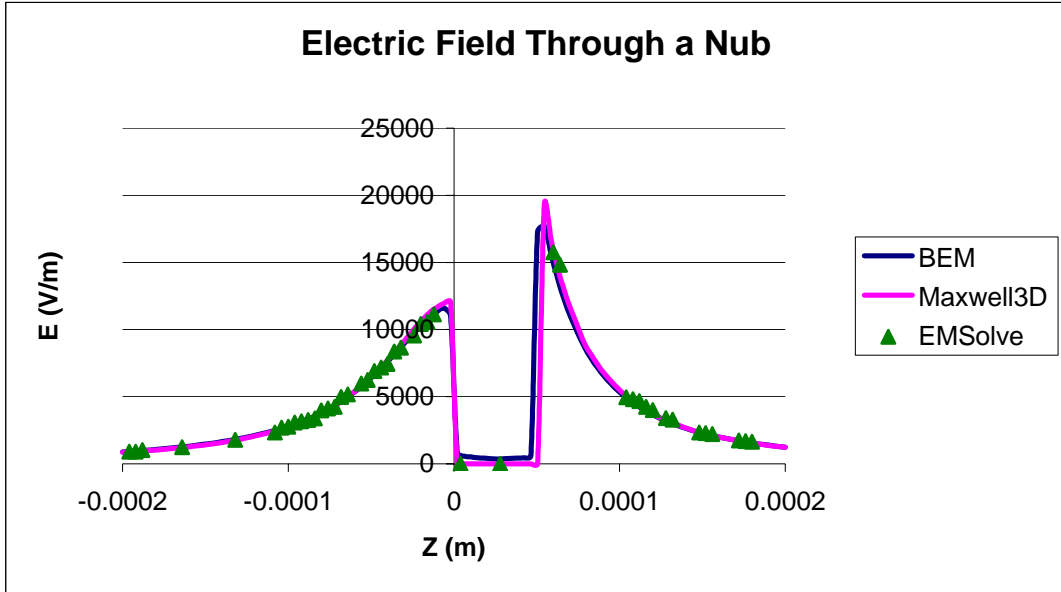


Figure 21. The magnitude of the electric field straight up through the +1 V nub.

The results for the maximum electric field magnitude and the breakdown voltage between the two spheres are shown in Table 2.

Table 2. Maximum electric field strength and breakdown voltage for the two nub problem.

	<i>BEMSTER</i>	<i>EMSolve</i>
Maximum Electric Field	33.7 kV/m	34.0 kV/m
Breakdown Voltage	178 V	177 V

PEC Disk in a Dome

The next model consists of a small PEC disk sitting above a dielectric. The dielectric and disk are enclosed in a metal case. The disk is a cylinder with rounded edges; the diameter of the cylinder is 1.016 mm, with height 0.1016 mm, and rounded

edges of radius 0.0508 mm. The bottom of the disk is flush with the top of the dielectric. This geometry is shown in Figure 22. Due to the difficulty of creating a volume mesh for this structure, only the BEMSTER code was used. The PEC disk was set to a potential of 1 V, while the outside conductors were set to 0 V. The mesh of the outside of the object is shown in Figure 23. The charge density on the PEC disk is shown in Figure 24.

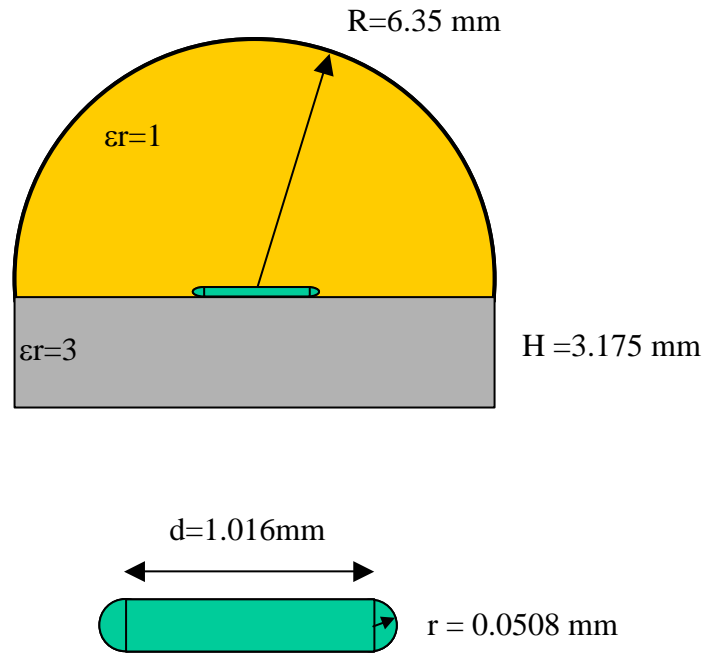


Figure 22. A PEC disk inside of a conducting dome.

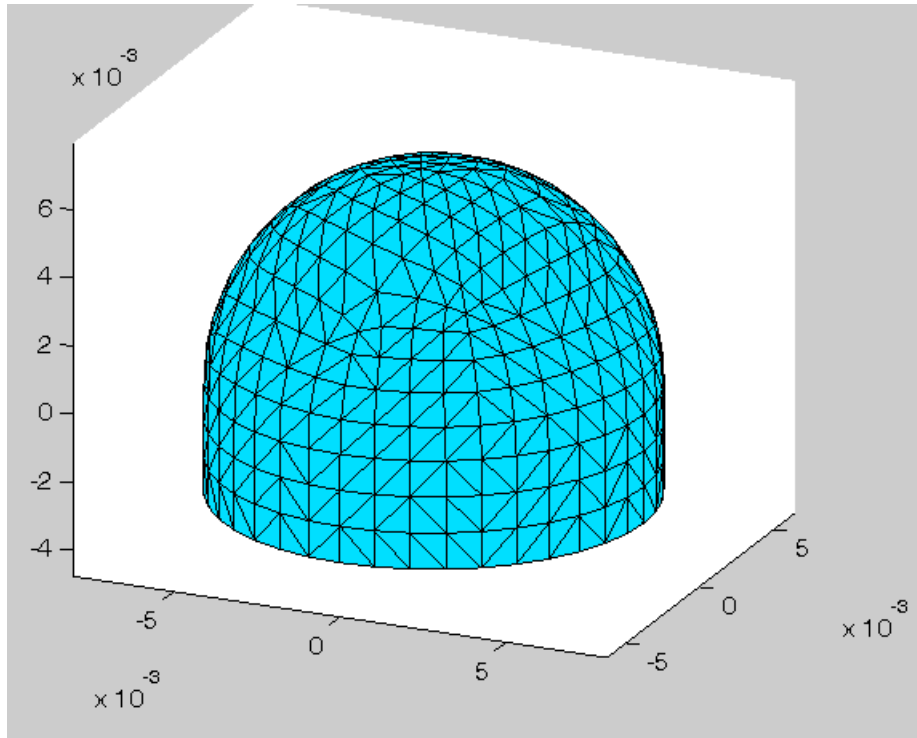


Figure 23. The surface mesh of the outside of the structure.

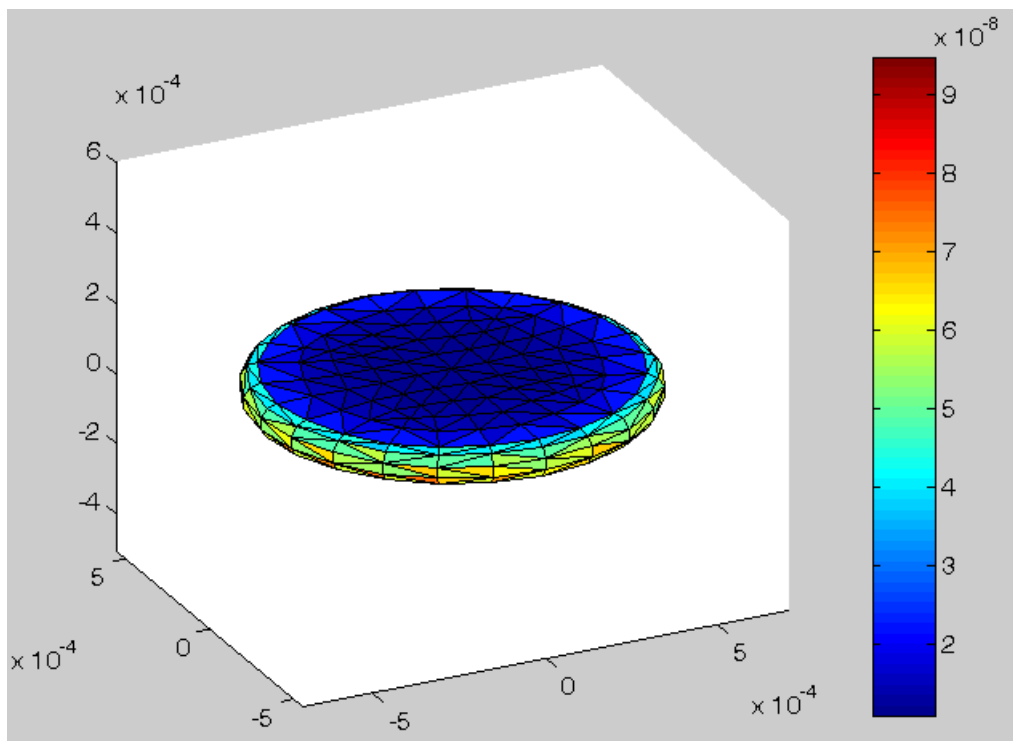


Figure 24. The charge density on the conducting disk.

Both the charge density plot and the electric field magnitude, shown in Figure 25, appear reasonable, with the majority of the charge accumulating on the edges of the disk. The maximum electric field can be calculated from equation 14 as $1.0715e+004$ V/m, leading to a breakdown voltage of 280.0 V between the disk and the outer shell.

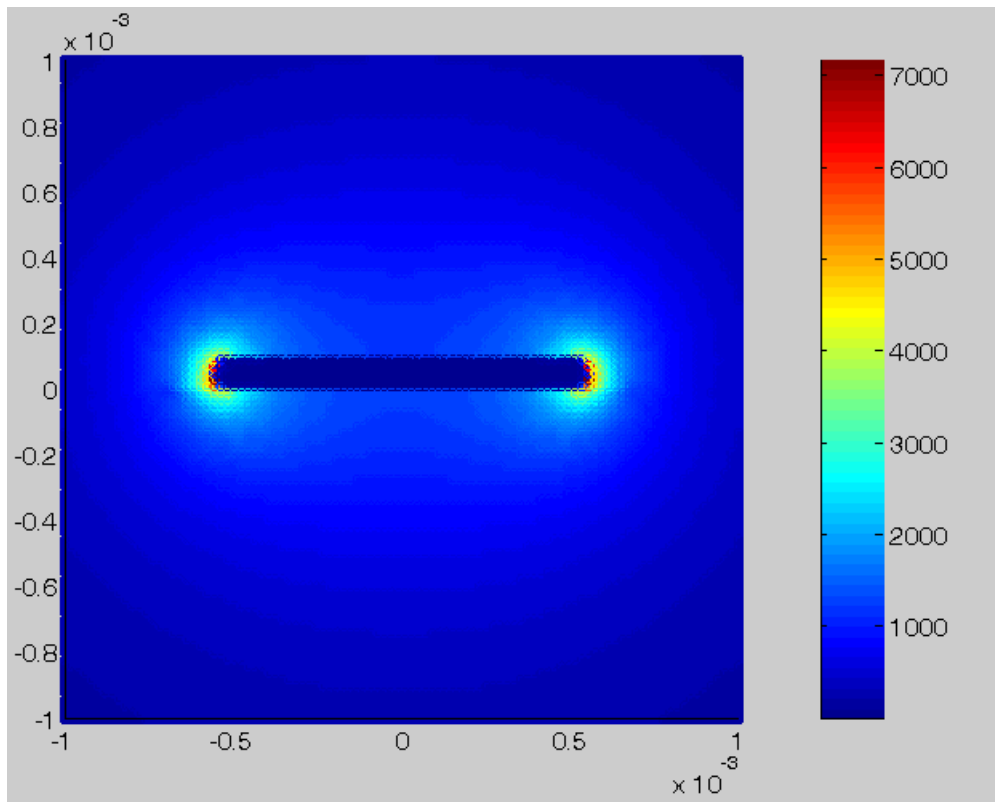


Figure 25. The magnitude of the electric field in the xz plane.

V. Conclusions

The EMSolve finite-element code and the BEMSTER boundary-integral code have been successfully used to simulate dielectric breakdown problems for structures

containing combinations of dielectrics and conductors. Both codes were compared to analytic solutions for simple problems and shown to have good agreement. They were then used to analyze several structures to see how much voltage would cause dielectric breakdown. EMSolve was found to have easier post-processing capabilities, while BEMSTER had easier mesh generation.

VI. References

- [1] Rao, S. M., Sarkar, T. K., Harrington, R. F., “The Electrostatic Field of Conducting Bodies in Multiple Dielectric Media,” *IEEE Transactions on Microwave Theory and Techniques*, November 1984, pp. 1441-1448.

- [2] Rao, S. M., Sarkar, T. K., “Static Analysis of Arbitrarily Shaped Conducting and Dielectric Structures,” *IEEE Transactions on Microwave Theory and Techniques*, August 1998, pp. 1441-1448.

- [3] White, J., Tausch, J., “Capacitance Extraction of 3-D Conductor Systems in Dielectric Media with High-Permittivity Ratios”, *IEEE Transactions on Microwave Theory and Techniques*, January 1999, pp. 18-26.